Dynamic Wireless Charging of Electric Vehicle: Misalignment Detection using Sensor Coils

- Capstone II -

Project Report

Nazarbayev University
Department of Electrical and Computer Engineering
School of Engineering and Digital Sciences

NAZARBAYEV UNIVERSITY

Electrical and Electronics Engineering
Nazarbayev University
http://www.nuece.info

Title:
Dynamic Wireless Charging of Electric Vehicle: Misalignment Detection using Sensor Coils

Theme:
Electric Vehicle

Project Period:
Spring Semester 2020

Project Group:
N/A

Participant(s):
Daryn Negmetzhanov
Yeldos Dauletkhanuly

Supervisor(s):
Professor Mehdi Bagheri
Professor Amin Zollanvari

Copies: 1

Page Numbers: 15

Date of Completion:
April 25, 2020

Abstract:

Precipitous development and commercialization of Electric Vehicles (EVs) become state of art technology. Likewise, demand for rapid feeding operation like Dynamic Wireless Charging (DWC) system is enhancing. Nevertheless, drawback in the form of misalignment between charging coil and receiver side attenuates standing of the DWC. Many studies were conducted to accomplish the throughput of this technology based on various aspects. In some articles, coil shape is the primary aim, while others concern with wireless power transfer (WPT) circuit. The fundamental aim of this project is to elevate the efficiency of the DWC by eliminating misalignment issue between source and load coils. It will cover background of the DWC with moderate literature review followed by own proposed methodology. The suggested topology was first simulated in the ANSYS Electronics software, then PSIM was applied to test is in hardware. Obtained results used in the overall system simulation show promising outputs.

Contents

Chapter 1

Introduction

1.1 DWC of EV

Advent of global warming issue and air pollution challenge forced industry to alter the way of thinking. Such enormous change is highly observed in transportation sector, where manufacturers gradually move toward zero-emission car production. At the beginning of the XXI century, hybrid electric vehicles (HEV) were innovative solutions in the world. However, according to the annual report in 2015 of the International Energy Agency (IEA) , only 1.5% of the total annual vehicle production was HEV. Moreover, the vast majority of them applicable only in "innovative market" such as USA and Japan. Therefore, EVs without fuel engine are state of art technology. Initially, EV could be charged only at charging stations using physical connection. Drawbacks in terms of charging time and the battery storage size, which influences cost of the car, brought modern solution of recharging called wireless charging system (WCS). They were simple, more reliable and cheaper, nevertheless stationary charging only in a specific parking areas and traffic signals diminished its usability in a wide-scale. Therefore, dynamic wireless charging (DWC) of the EVs were introduced, which stands for that car can be charged during the motion.

1.2 DWC Advantages and Drawbacks

DWC can be achieved by applying the principle of Wireless power transfer (WPT) technology in the feeding operation, where car get energy without physical connection. It enables automatic charging of the vehicles in three various ways such as static (SWC), quasi-dynamic (QWC) and dynamic (DWC) [1]. The former one has advantage in terms of lack of hazards arising from wires and flexibility to be integrated in conventional whereabouts. QWC is applicable where charging for short period is required such as during the traffic light stops or parking areas. Superiority of the DWC is increased travelling range and reduced battery size followed by the reduction in the cost of the vehicle itself. The latter method is the most demanding in the industry due to before mentioned aspects [1].

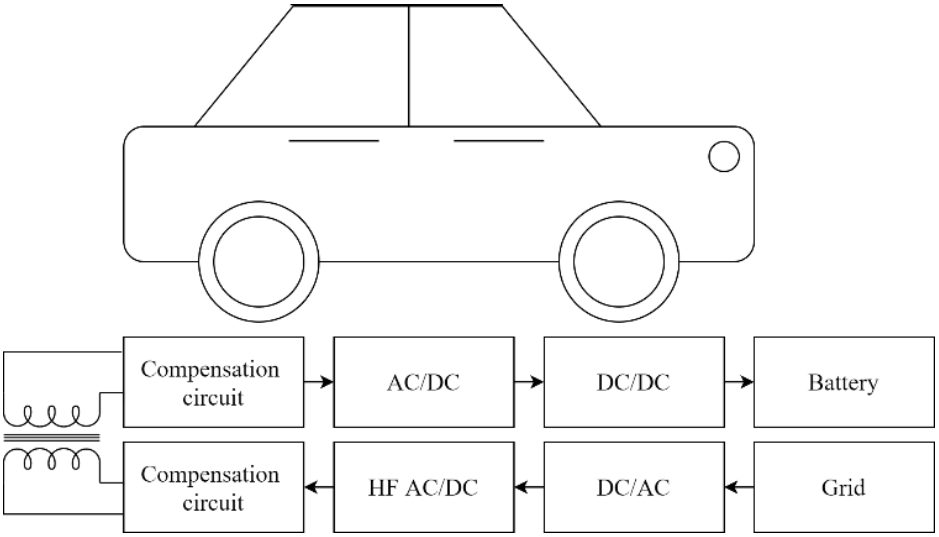

Figure 1.1: DWC operating principle from the grid to the battery

The general illustration (see next chapter for detailed) of the wireless charging can be observed from the Figure 1.1. It consists of different block parameters starting from grid which is the source of energy followed by AC to DC converter. After that half-bridge circuit transforms DC to AC and compensation circuit increases diminished power efficiency where further WPT occurs. On the receiver side the same procedure happens with opposite direction.

Properties affecting the throughput of the aforementioned WPT, especially DWC, are various, however the main drawbacks of the DWC system are the misalignment between transmitter and receiver coils and air-gap between them [2]. In order to achieve supreme power transfer from the source to the vehicle battery, a certain range of the alignment has to be adhere. Trying to obtain perfect lining is arduous even for trained driver, which will distract person from the traffic that will have tremendous issue. [3]. Many scientific works were implemented to solve this issue. [4] suggested MR sensor based solution to detect misalignment. However, this methodology is applicable only in static wireless charging case. Ruddell et.al proposed modern topology for DWC with integrated energy storage. The drawback of this system is the complexity of the network and cost. One of the recent works were done by Cirimele et al [5], however they have considered platform for charging, not the vehicle itself. [6] studied impact of loading conditions on the DWC performance. Nevertheless, they applied only series-series network for testing case. Therefore, this project intends to propose modern solution with additional low cost coils.

Chapter 2

Theory and Analysis

2.1 Optimal WPT Topology

Power between transmitter and receiver side can be altered and improved according to the different WPT circuit combinations. Regarding to the [7], there are mainly four types of the WPT topologies: inductive, capacitive, magnetic gear and resonant inductive. Each of the methods has own benefits and operating principles which is summarised in the table 2.1. As it can be observed, some topologies have medium efficiency, at the same lower price. According to the designer decision and application purpose these topologies will be opted for.

Another factor affecting the performance of the DWC of EV is the hardware of the system. Generally, it contains rectifiers, inverters, drivers and etc (detailed explanation of the hardware will be covered in the next chapter). One of such elements in the network is the compensation circuit. It is used in order to increase the efficiency of the power on the secondary side. Usually, two compensation circuits are applied for single pair of energy transformation, where one is located on the transmitter side and other one in the receiver coil side. The most recent research on compensation was conducted by Huang et. al. They in depth had considered the relationship between compensation network and

WPT topology	Efficiency	Frequency range(kHz)	Power level	Price	Size
Inductive	High	10-50	Medium\High	Medium\High	Medium
Capacitive	Medium	100-600	Low	Low	Low
Permanent magnet	Low	0.05-0.5	Medium	High	High
Resonant inductive	Medium	10-150	Medium\Low	Medium	High

Table 2.1: Characteristics of different WPT topology

Compensation circuit	Power transfer	Sensitivity to air-gap	Misalignment tolerance	Application in EV
Series-series	High	Less	High	High
Series-parallel	High	Less	High	High
Parallel-series	Low	Medium	Medium	Medium
Parallel-parallel	Low	Medium	Low	Medium

Table 2.2: Characteristics of different compensation circuit combinations

power efficiency of an series and series-parallel network [8]. Also, they had implemented design methodology to optimize power efficiency and restrict output sensitivity. According to the [9], there are two possible combinations for the transmitter coil such as series and LCL, while there are three ways of compensation on the secondary side like series, parallel and LCL. Table 2.2 provides data regarding to the general combination of different compensation network.

In order to show relationship between power rating and mutual inductance during the energy transformation, the simplest circuit of WPT will be taken. The source voltage in this circuit can be determined as in (2.1), while load coils as in (2.2):

$$V_S = (R_S + \frac{1}{j\omega C_S} + j\omega L_S)I_1 - j\omega M I_2 \tag{2.1}$$

$$(R_L + \frac{1}{j\omega C_L} + j\omega L_L)I_2 - j\omega M I_1 = 0 \tag{2.2}$$

where R_S (R_L), C_S (C_L) and L_S (L_L) represents resistance, capacitance and inductance for source and load respectively. V_S is the source voltage, AC in this case, whereas ω with M stands for angular frequency and mutual inductance between transmitter and receiver side. Finally, applying KCL and KVL laws, one can determine the obtained power on the load side of the coil:

$$P_L = I_L^2 R_L = |\frac{-\omega^2 M^2}{[(R_S + \frac{1}{j\omega C_S} + j\omega L_S)(R_L + \frac{1}{j\omega C_L} + j\omega L_L) + \omega^2 M^2]^2}| V_S^2 R_L \tag{2.3}$$

Detailed study of the derivation of the equations can be found on [10].

2.2 Misalignment Issue

As the main objective of the project is to solve misalignment issue during the energy transformation, this section will give a brief explanation on this challenge. There are sundry types of the misalignment such as lateral, angular, rotational. According to the [11], the former one is the most decisive fact that influence power performance on the load

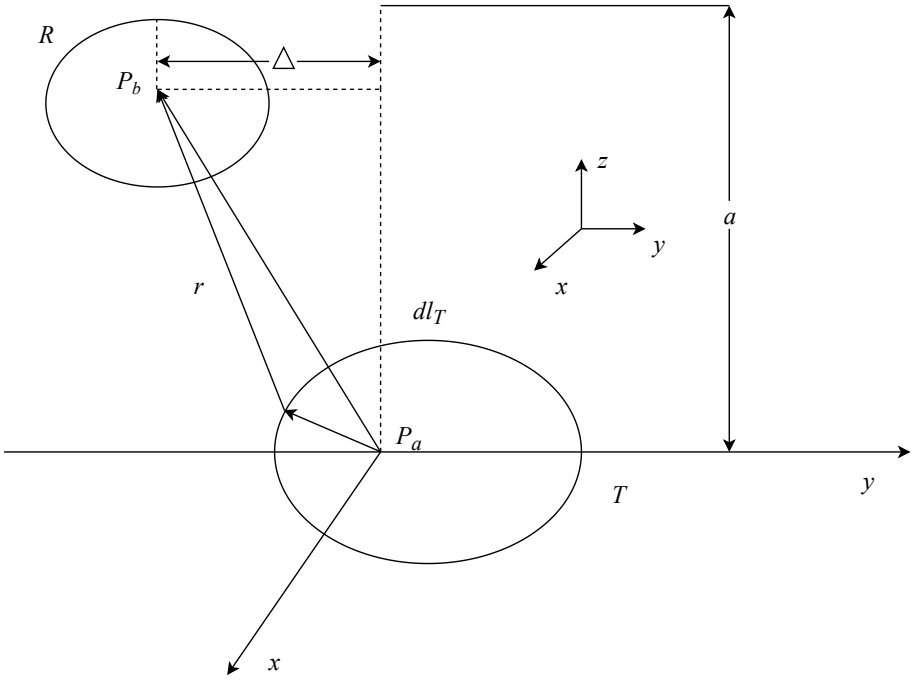

Figure 2.1: Lateral misalignment between transmitter and receiver coils

side. Therefore, this project will consider the lateral misalignment only, Figure 2.1, while thorough analysis on the remaining is applicable on [3].

Applying the Ampere's law [12] for closed path:

$$\oint B\,dl = \mu_0 N I \tag{2.4}$$

where B is the magnetic flux, μ_0 is the permeability constant, N is the number of turns and I is the current. Also, from the Figure 2.1 the magnetic field intensity derived as:

$$H = \frac{I_T}{4\pi} \sum_{i=1}^{n} \frac{a_i^2}{2\sqrt{(a_i^2 + \Delta^2)^3}} \tag{2.5}$$

where I_T is the transmitter side current and other parameters shown in the Figure 2.1. Moreover, the magnetic flux density (B) in terms of the voltage can be computed by applying the Faraday's law [13]:

$$V_i = -\frac{d}{dt} \oint B\,ds \tag{2.6}$$

and signifying B with field strength:

$$B = \mu H = \mu_0 \mu_r H \tag{2.7}$$

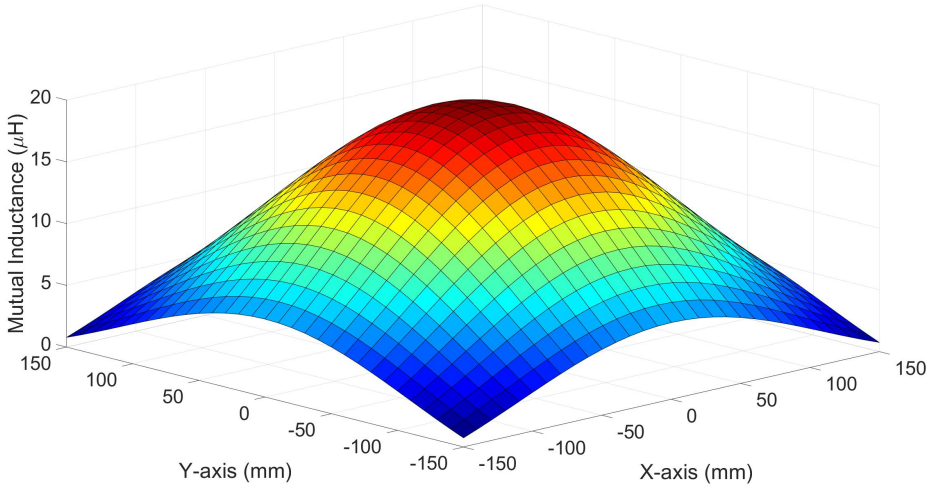

Figure 2.2: Variation of mutual inductance value regarding to the misalignment over y-axis and x-axis

with combining the equations (2.10), (2.12) and putting into (2.11), one can achieve pick-up voltage formulation:

$$V_i = j\mu_0\omega H \sum_{j=1}^{k} \pi b_j^2 \tag{2.8}$$

while b_j is the radial length of the receiver coil. Equation (2.13) states that induced voltage on the load coil side is directly proportional to the arising magnetic field strength. While H itself indirectly related to the Δ (1.10) which is the lateral misalignment between charging and pick-up coils. Therefore, mathematical computation exhibits that higher lateral misalignment leads to decreased induced voltage, which also cause reduction in power on the receiver coil (2.6). In order to visualize this pattern, refer to the (2.8) where mutual inductance value is positively correlated with load power. Thus, inductance between source and load will be diminished if the power does so which is dependent on the misalignment value. Figure 2.2 illustrates aforementioned conclusion. It shows position of transmitter and receiver with respect to each other over x-axis and y-axis. It can be clearly observed that during the perfect alignment, M has the maximum available value, whereas it attenuates across broad area of the misalignment reaching the lowest point on the 150mm on both axis.

Chapter 3

Proposed methodology

3.1 Coil Models

Due to the dynamic mutual inductance existence in DWC, the voltage level of the receiver is not helpful for identifying the misalignment [14]. Two sensor coils were proposed in the Capstone I, which will have different voltage levels at misalignments due to non-equal distances [15]. Figure 3.1 depicts the configuration of the model of proposed methodology and is viewed for the simulation in the Ansys Maxwell software. The larger bottom and top coils are transmitter and receiver coils respectively, whereas two small coils are sensor coils. For the scope of the DWC, two coils are enough as neither front nor rear misalignment needs to be discriminated.

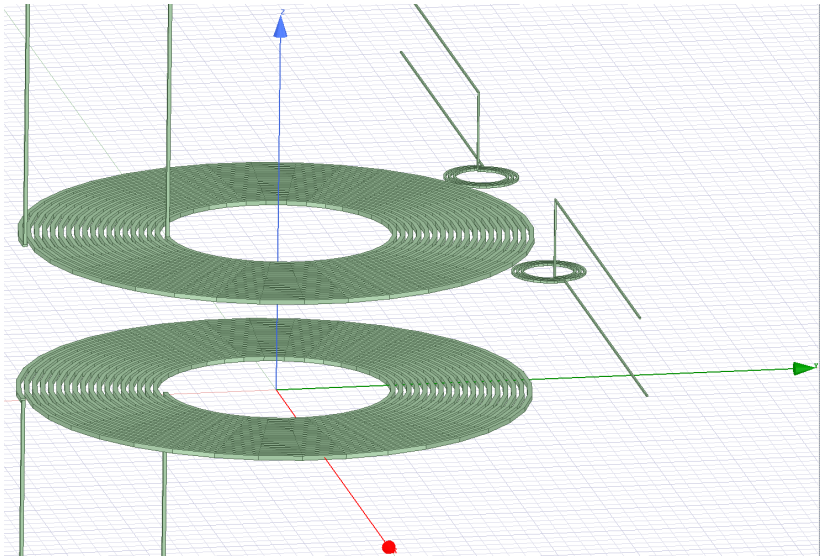

Figure 3.1: Simulation Model

3.2 System Model

In order to test usability and effectiveness of the coil model, the real-life case hardware is needed, however, only software simulation of circuit was constructed as shown in Figure 3.5. In this circuit (1) DC power is converted to AC power, (2) AC power is passed due to mutual inductance from primary (transmitter) to secondary (receiver side), (3) AC power is converted back to DC power fed into the battery. The elements, their significance and responsibilities in the system are as follows:

- Microcontroller. The microcontroller generates the pulses, which are used as drivers input. Also, the microcontroller is capable to read the voltage level of sensor, and identify the direction of turn to align the receiver with transmitter.

- Driver. The IGBT based inverters and Power Mosfets used for the inverter and DC/DC boost converter need the driver to control their gates, as specific voltage level is required, which is not maintained by the microcontroller in real-life hardware setup scenario, however, this is out of the scope of the simulation.

- Inverter. For obtaining high-frequency AC signal (for power transfer 20kHz is treated as high frequency), the inverter controlled by driver is vital. For the hardware implementation IGBT based H-bridge converter is suggested and is used in the simulation. Two drivers are required to input complementary signal, e.g. when one driver is at state V_{cc}, the other is at state 0.

- Compensation network. The power transfer efficiency through inductive coupling is highly contingent upon the reactance level at utilized frequency, whereas the compensation network gives opportunity to transfer power at uttermost efficiency, if values are correctly computed and constructed. The LCL-N topology showed relatively high performance at its low cost due to utilization of only single inductive load in series (3.1) and capacitive load in parallel (3.2) connected to the transmitting coil. In theory, this topology is most desired to the scope of our project as instead of connecting the compensation network to 4 coils (transmitter, receiver, 2 sensor coils), single compensation will be enough to achieve good performance of power transfer to receiver and coil sensors. The efficient power transfer to sensor coils is also desired as voltage levels should be high enough to be differentiated.

$$L_{series} = L_{tx} \tag{3.1}$$

$$C_{parallel} = \frac{1}{w_0^2 L_{tx}} \tag{3.2}$$

- Rectifier. Only DC power is fed into the battery, thus received AC at the secondary side is converted to DC by the rectifier. For rectifier the full-wave rectifier with capacitor for smoothing is proposed. However, the output of the rectifier will vary

due to the nature of DWC, where mutual inductance is dynamic and voltage levels vary.

- Closed loop DC/DC Boost converter. The battery should be always charged at voltage rate of 1-2 V higher than the battery's rated voltage for increasing the number of battery cycles. For the purpose of stabilizing the voltage, closed loop DC-DC boost converter with capacitor is proposed, which can result in stable voltage, hence elongation of battery life. The closed loop is controlled by changing the duty cycle and the frequency of gate, which is microcontroller's burden, and the voltage gain is as follows:

$$V_{out} = \frac{V_{in}}{1 - D}, \tag{3.3}$$

where

$$D = \frac{t_{on}}{t_{on} + t_{off}} \tag{3.4}$$

The DC/DC boost converter is not the only option to resist the voltage pulsations, which are detrimental for the battery. The use of ultracapacitors connected in parallel to the battery is feasible, or supercapacitors even are able to replace the batteries, but this is subject to experiments during the real-life hardware setup. Otherwise, the separate battery management system (BMS) of the battery could be also utilized for obtaining high-quality control during the charging of the battery at appropriate voltage and current. It should be noted that the possible expenses for the proposed implementation of hardware setup were tried to be minimized and the hardness of the construction lightened to be feasible for contruction.

3.3 Simulation and Results

From quantitative analysis, the correlation of power or voltage and mutual inductance is direct proportionality. The simulation, thus, considers mutual inductance for the verification of the theory. The coil parameters were chosen as in [16] for the main coils and the dimensions of the peripheral sensor coils are arbitrary, however, more turns and larger diameter of conductors will induce larger voltage which is undesired for the sensor coils which results in power loss of the receiver.

Two simulations with and without the sensor coils were done to prove the negligent disturbance of the sensor coils on the WPT (see Figure 3.2). Another desired feature of the sensor coils is precision. The simulation's purpose is to show that voltage induced inside the sensor coils due to transmitter are different. Figure 3.3 shows that the mutual inductance between sensor coils and transmitter, with increase of mutual inductance for left sensor coil while shift is to the right direction and vice-versa for right sensor coil. At no misalignment, however, the intersection does not occur due to unsymmetrical nature of the coils during the simulation. If this is the case for the hardware, then calibration

Table 3.1: Coil Parameters

Parameter	Transmitter and Receiver Coils	Sensor Coils
Number of Turns	18	3
Inner Diameter	140 mm	30 mm
Conductor Diameter	4 mm	2 mm
Turn spacing	1 mm	1 mm
Outer Diameter	320 mm	24 mm

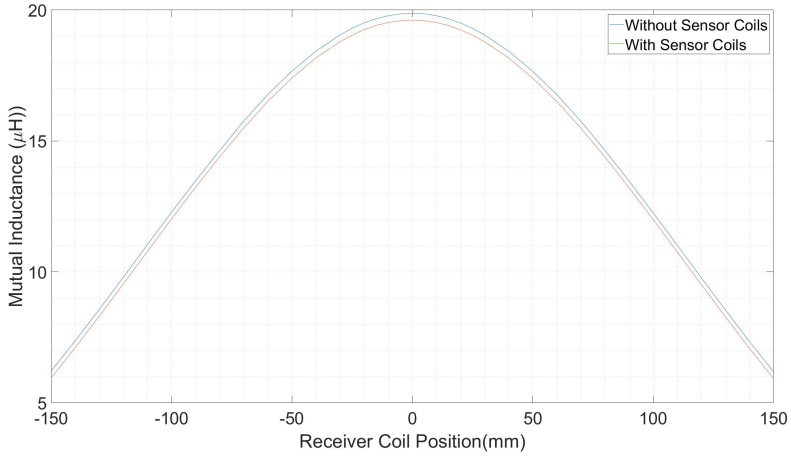

Figure 3.2: Mutual Inductance between Receiver and Transmitter with and without Sensor Coils

or offset could be taken for consideration while identifying the direction of misalignment. Figure 3.4 shows how the direction to align perfectly is identified, e.g. by considering negative mutual inductance, hence negative voltage result shows the direction to align as right, and vice-versa for positive voltage.

The simulation of the system was implemented in PSIM software, which is suitable for the simulation of power electronics circuits. The purpose of the simulation is to ensure the proper operation of the whole system. For simulation to be sound with sensor coils model, the results of in Section 3.3 were used for self and mutual inductance, both for testing with the receiver and sensor coils. The parameters were chosen as discussed in previous section for LCL-N compensation network, whereas the capacitance values for rectifier and DC-DC boost converter were approximated. Overall, the simulation improvements as well as the selection of more precise values for components is desirable. The circuit used for the simulation can be seen from Fig.3.5, the simulation scenario is different from the real-life scenario, so that during simulation the control circuit used for the closed loop DC/DC boost converter is made using PID (refer to figure 3.6).

Since PSIM requires only gate blocks to be wired to the gate junction of the IGBT mod-

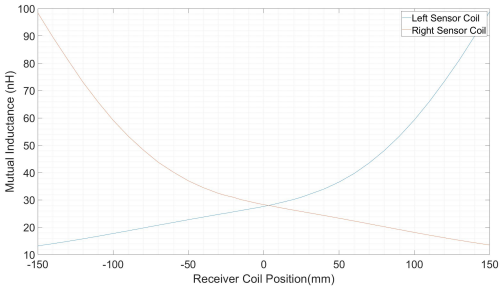

Figure 3.3: Mutual Inductance between Right, Left Sensor and Transmitter Coils

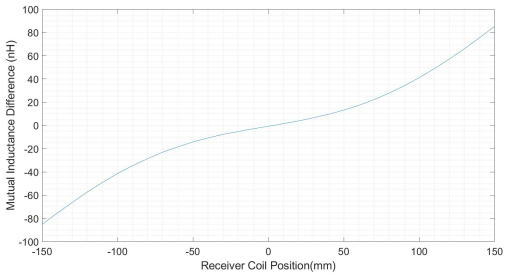

Figure 3.4: Mutual Inductance of Left Sensor Coil subtracted by Mutual Inductance of Right Sensor Coil

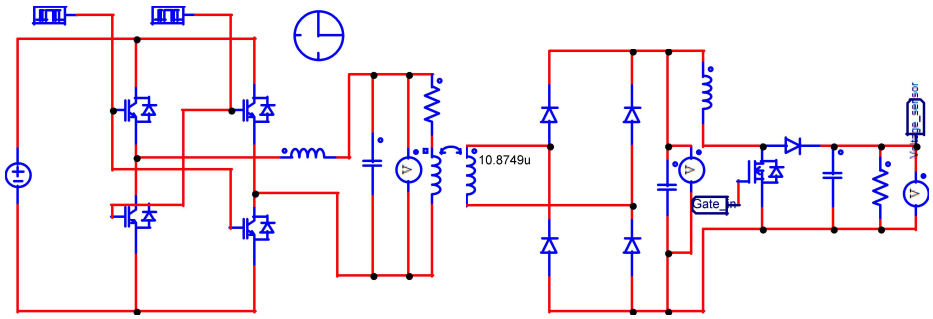

Figure 3.5: Schematic of simulation for proposed system

ule, two different gating blocks, such that all values of 2nd gate block equals *NOT* 1st gate block values, are configured with 20kHz frequency; instead of creating logic elements, which eventually will bring to same results. The proposed system's simulation with 300 Volts DC source input results with different mutual inductance seen in Figure 3.2. The output of the rectifier is 20kHz AC signal, which coincides with the theory. Figure 3.8 shows the voltage after the DC/DC boost converter at different mutual inductance. The utilized mutual inductance in the figure are 12μH, 16μH and 19.88μH at 100 mm, 75 mm and 0 mm misalignment respectively. The deterioration of mutual inductance values between transmitter and receiver increases after 30 mm misalignment. At this misalignment

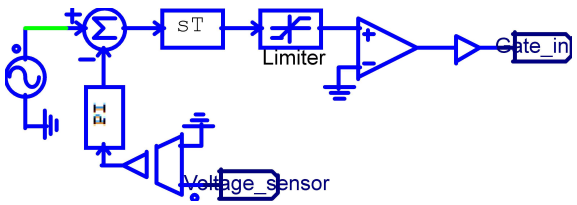

Figure 3.6: Control circuit of DC/DC boost converter

to the left side, the voltages induced in the sensor coils can be seen in figure 3.9. With larger misalignment rises, whereas for the small deviations from alignment accurate voltage sensors are required.It also should be noted that this voltages will vary mainly due to the varying mutual inductance during the motion of the receiver, however, the voltage sensors at sensors coils should be as precise as to distinguish the voltage difference of 10mV. The lowest and highest values to be seen by the voltage sensor at the sensor coils is from approximately 0.015V to 0.18V (refer to figure 3.10).

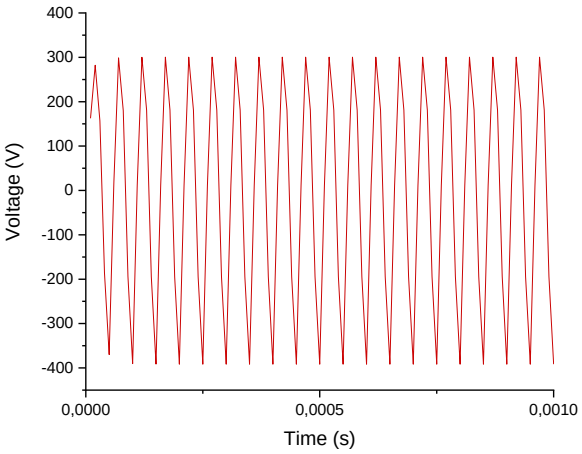

Figure 3.7: Output voltage of Inverter

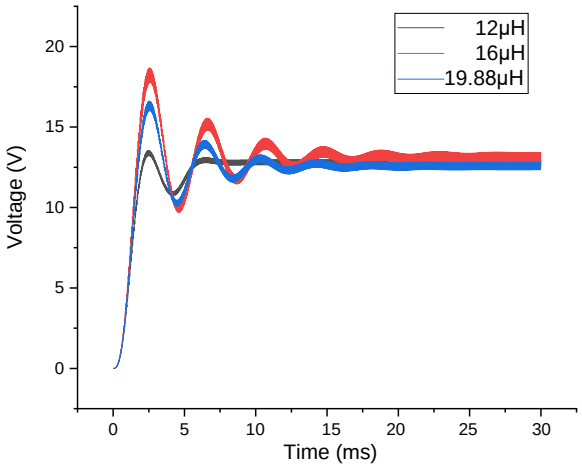

Figure 3.8: Output Voltages of closed loop DC/DC boost converter at different mutual inductance

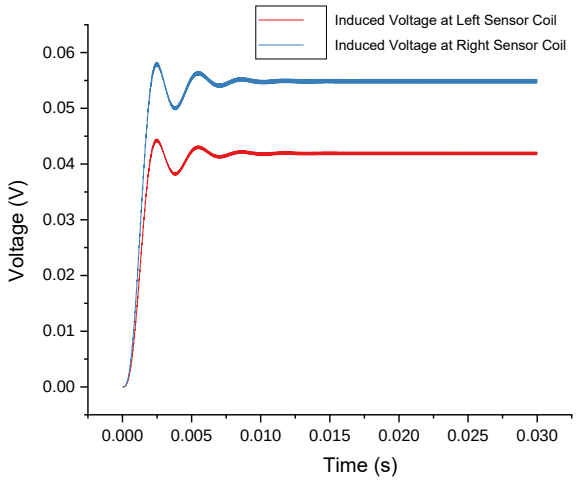

Figure 3.9: Voltage Induced in Sensor Coils at 30 mm misalignment

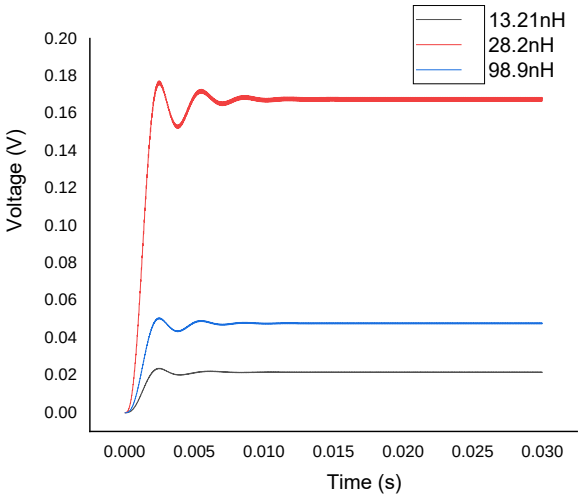

Figure 3.10: Voltages induced at 150mm misalignment to the left, perfect alignment, 150mm misalignment to the right in the left sensor coil

Chapter 4

Conclusion

Optimal methodology for lateral misalignment detection with sensor coils was proposed during the Capstone I and simulation was conducted according to the previous studies design parameters. The obtained results prove the analytical analysis and ability of the new method to eliminate misalignment challenge to some extent. In addition, the performance of the topology can be enhanced by applying suitable WPT circuits, which was mentioned before. Also, the shape of the receiver and transmitter during this project is taken as circular, while there is a possibility to integrate other coil forms such as rectangular and so on.

The primary aim for the Capstone II is to construct practical coils and conduct a test for the efficiency. In order to do that various equipment including software application are required.[17]

Bibliography

[1] X. Mou et al. "Survey on magnetic resonant coupling wireless power transfer technology for electric vehicle charging". In: *IET Power Electronics* 12.12 (2019), pp. 3005–3020.

[2] K.A. Kalwar et al. *Coil Design for High Misalignment Tolerant Inductive Power Transfer System for EV Charging*. 2016.

[3] A. Ahmad and M.S. Alam. "A Comprehensive Review of Wireless Charging Technologies for Electric Vehicles". In: *IEEE Transaction on Transportation Electrification*. 2018.

[4] T. V. Jeshma and B. George. "MR Sensor-Based Coil Alignment Sensing System for Wirelessly Charged EVs". In: *IEEE Sensors Journal* 20.10 (2020), pp. 5588–5596.

[5] V. Cirimele et al. "The Fabric ICT Platform for Managing Wireless Dynamic Charging Road Lanes". In: *IEEE Transactions on Vehicular Technology* 69.3 (2020), pp. 2501–2512.

[6] H. H. Kabalan et al. "The Impact of Coupling and Loading Conditions on the Performance of S-S EV Dynamic Wireless Charging Systems". In: *2019 International Conference on Electrical and Computing Technologies and Applications (ICECTA)*. 2019, pp. 1–5.

[7] Chirag Panchal and Sascha Stegen. "Review of static and dynamic wireless electric vehicle charging system". In: *Engineering Science and Technology, an International Journal* 21 (June 2018). DOI: 10.1016/j.jestch.2018.06.015.

[8] Z. Huang et al. "Design of Series/Series-Parallel Compensated Inductive Power Transfer Converter as Wireless Grid to Vehicle Interface". In: *2019 IEEE Vehicle Power and Propulsion Conference (VPPC)*. 2019, pp. 1–5.

[9] Y. Zhang et al. "A High-Power Wireless Charging System Using LCL-N Topology to Achieve a Compact and Low-Cost Receiver". In: *IEEE Transactions on Power Electronics* 35.1 (2020), pp. 131–137.

[10] Alireza Dayerizadeh. *Dynamic Wireless Charging for Electric Vehicles: Approaches for Reflexive Field Containment Using Reactive Components*. Jan. 2020. DOI: 10.13140/RG.2.2.11643.67369.

[11] Y. Gao et al. “Misalignment effect on efficiency of wireless power transfer for electric vehicles”. In: *2016 IEEE Applied Power Electronics Conference and Exposition (APEC)*. 2016, pp. 3526–3528.

[12] E. R. Williams and P. T. Olsen. “A Method to Measure Magnetic Fields Accurately Using Ampere’s Law”. In: *IEEE Transactions on Instrumentation and Measurement* 27.4 (1978), pp. 467–469.

[13] A. E. Umenei, Y. Melikhov, and D. C. Jiles. “Analytic Solution for Variations of Magnetic Fields in Closed Circuits: Examination of Deviations From the “Standard” Ampere’s Law Equation”. In: *IEEE Transactions on Magnetics* 47.4 (2011), pp. 734–737.

[14] D. Kishan and P. S. R. Nayak. “Wireless power transfer technologies for electric vehicle battery charging — A state of the art”. In: *2016 International Conference on Signal Processing, Communication, Power and Embedded System (SCOPES)*. 2016, pp. 2069–2073. DOI: 10.1109/SCOPES.2016.7955812.

[15] Raymond A. Serway and Chris Vuille. *Essentials of college physics*. Thomson-Brooks/Cole, 2007.

[16] Ainur Rakhymbay et al. “Precise Analysis on Mutual Inductance Variation in Dynamic Wireless Charging of Electric Vehicle”. In: *Energies* 11 (Mar. 2018), p. 624. DOI: 10.3390/en11030624.

[17] Ivan Cortes. “Automatic Positioning System for Inductive Wireless Charging Devices and Application to Mobile Robot”. MA thesis. Texas A M University, 2007.